The following publication Y. Yang, H. W. Rebecca Liang, S. C. Tan and S. Y. Ron Hui, "Design of A Wireless Power Modulator for Wireless Power Transfer Systems," 2021 IEEE 12th Energy Conversion Congress & Exposition - Asia (ECCE-Asia), 2021, pp. 816-820 is available at https://doi.org/10.1109/ECCE-Asia49820.2021.9479411

Design of A Wireless Power Modulator for Wireless Power Transfer Systems

Yun Yang[1], Hui Wen Rebecca Liang[2], Siew Chong Tan[2], and Shu Yuen Ron Hui[3,4]
[1]Department of Electrical Engineering, The Hong Kong Polytechnic University, Hong Kong, China
[2]Department of Electrical and Electronic Engineering, The University of Hong Kong, Hong Kong, China
[3]Department of Electrical and Electronic Engineering, Nanyang Technological University, Singapore
[4]Department of Electrical and Electronic Engineering, Imperial College London, London, U.K.
Email: yun1989.yang@polyu.edu.hk[1], u3004844@connect.hku.hk[2], sctan@eee.hku.hk[2], ron.hui@ntu.edu.sg[3]

***Abstract*-This paper presents the design guidance of a wireless power modulator (WPM) for wireless power transfer (WPT) systems with multiple receivers. The WPM is implemented by an inductive-dominant relay resonator to alter the transimpedances among the receivers through the processes of enhancing, decoupling or weakening the magnetic flux in the receivers. The proposed WPM can manage the power flow of WPT systems without any control and communication devices, which improve the reliability and cost-efficiency. A 20 W WPT system with two LED loads is set up to demonstrate the effectiveness of the proposed WPM in regulating the power flow. The WPT system operates at 100 kHz.**

***Index Terms*—Wireless power modulator (WPM), wireless power transfer (WPT), power flow, transimpedance.**

I. Introduction

The concept of power decoupling (PD) technique is not new. It has been widely adopted in microwave applications at Giga-Hertz operations to reduce coupling between outputs ports or antennas [1]. A common example is the power divider pioneered by Ernest J. Wilkinson in 1960 [2]. A Wilkinson power divider can decouple multiple output ports while maintaining a matched condition on all these ports so that waves can only propagate between the input and output port with reduced or no interference to other output ports.

However, existing PD techniques that have been adopted in microwave applications are unsuitable for WPT applications with charging power in the range from typically 5 W for mobile phones to 50 kW for electric vehicles (even though it was suggested for WPT at 5.8 GHz for very-low-power (milli-watt) applications in [3]). There are three major reasons:

1. These Giga-Hertz methods are based upon wave propagation principle involving impedance matching with the power source, and this do not fit into the transmission frequency range of 85 kHz to 13.56 MHz currently specified in WPT standards such as Qi, A4WP, and SAE [4-6]. The relatively low frequency operations in these standards do not exhibit wave properties in the energy transfer.
2. The need to match impedance with the power source in microwave PD techniques implies that the maximum power transfer theorem is used. It has been clearly pointed out in [7] that such approach will lose at least half of the input power in the source resistance, making it unsuitable for WPT of substantial power as the system energy efficiency will never exceed 50%.
3. The switching speed of modern power electronics cannot achieve Giga-Hertz operation. This means that there is no low-cost solution for developing medium-power or high-power Giga-Hertz operation for WPT applications.

To bridge the research gap, a new wireless power modulator (WPM) is proposed in this paper. Unlike the conventional power decoupler being designed for signal processing, the proposed WPM is designed for power regulations. Therefore, a conventional power decoupler designer may concern about the intensity of signals (i.e., SI unit is dB), whereas a WPM designer only consider the system power (i.e., SI unit is W). Besides, the WPM is more than a power decoupler. It can be adopted to enhance (or weaken) the output power by enhancing (or weakening) the magnetic flux of inductive coils.

In this paper, the WPM is implemented by an inductive-dominant resonator that can alter the transimpedances among the receivers. A systematic design guidance for the proposed WPM is provided. Experiments are conducted on a 20 W and 100 kHz WPT system with two LED loads and one WPM to verify the effectiveness of the design method. It is noted that the non-radiative WPT systems obey the same law of physics. Therefore, the proposed WPM should be available for WPT systems with multiple receivers operating in the frequency range of 85 kHz to 13.56 MHz, which is not within the wave propagation domain. Compared to the conventional power regulation schemes using control and communication devices for WPT systems with multiple receivers operating within the frequency range of 85 kHz and 13.56 MHz (which have been investigated over the last decade [8-19]), the WPM takes the advantages of higher reliability and lower costs from two perspectives:

1. It is well-known that the most popular peer-to-peer technology, i.e., Bluetooth and Near-Field Communication (NFC), may suffer from communication delays and packet loss. Besides, their transmitting and receiving devices need additional charge. However, the WPM is communication-free.
2. The micro-controller units (MCUs) used in the conventional power regulation strategies are more expensive than a passive LC resonator used as the WPM, particularly for a WPT system at the Industrial Scientific Medical (ISM) band (e.g., 6.78 MHz and 13.56 MHz).

II. Model of a Single-Transmitter-Multiple-Receiver WPT System with WPM

Fig. 1 shows the circuit diagram of a single-transmitter-multiple-receiver WPT system with multiple WPM. Both the transmitter and receivers of the WPT system adopt series-series (SS)-compensations. The WPM coils are implemented using simple *LC* resonant circuits.

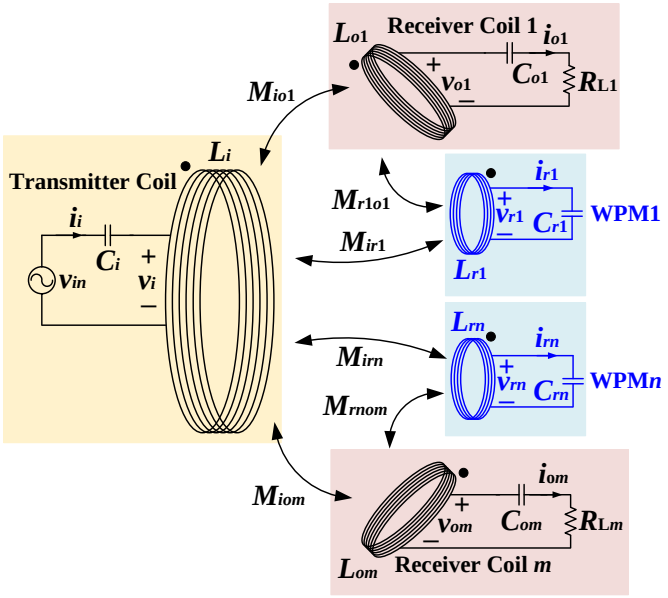

Fig. 1. Circuit diagram of a single-transmitter-multiple-receiver WPT system with multiple WPMs.

Based on the circuit diagram in Fig. 1, the equivalent circuit of the single-transmitter-multiple-receiver WPT system with multiple WPMs can be depicted as shown in Fig. 2.

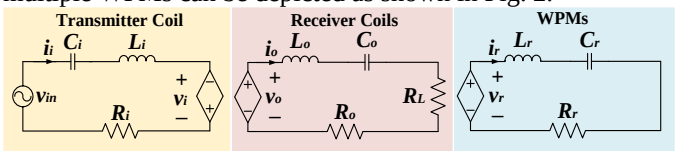

Fig. 2. Equivalent circuit of a single-transmitter-multiple-receiver WPT system with multiple WPMs.

The induced voltages of the transmitter coil (i.e., v_i), receiver coils (i.e., $\boldsymbol{v_o}$), and WPM (i.e., $\boldsymbol{v_r}$) can be expressed as

$$\begin{bmatrix}\overrightarrow{v_i}\\ \overrightarrow{\boldsymbol{v_o}}\\ \overrightarrow{\boldsymbol{v_r}}\end{bmatrix} = -j\omega \begin{bmatrix}0 & \boldsymbol{M_{io}} & \boldsymbol{M_{ir}}\\ -\boldsymbol{M_{oi}} & \boldsymbol{M_{oo}} & \boldsymbol{M_{or}}\\ -\boldsymbol{M_{ri}} & \boldsymbol{M_{ro}} & \boldsymbol{M_{rr}}\end{bmatrix}\begin{bmatrix}\overrightarrow{i_i}\\ \overrightarrow{\boldsymbol{i_o}}\\ \overrightarrow{\boldsymbol{i_r}}\end{bmatrix} \quad (1)$$

where ω is the operating angular frequency; r indicates the number of WPM coils, e.g., r_1 indicates the first WPM coil and r_2 indicates the second WPM coil; o_i indicates the number of receivers, e.g., o_1 indicates the first receiver and o_2 indicates the second receiver; $\overrightarrow{v_i}$ is the voltage across the transmitter coil; $\overrightarrow{\boldsymbol{v_r}} = \begin{bmatrix}\overrightarrow{v_{r1}}\\ \vdots\\ \overrightarrow{v_{rn}}\end{bmatrix}$ are the voltages across the WPM coils; $\overrightarrow{\boldsymbol{v_o}} = \begin{bmatrix}\overrightarrow{v_{o1}}\\ \vdots\\ \overrightarrow{v_{om}}\end{bmatrix}$ are the voltages across the receiver coils; $\overrightarrow{i_i}$ is the transmitter current; $\overrightarrow{\boldsymbol{i_r}} = \begin{bmatrix}\overrightarrow{i_{r1}}\\ \vdots\\ \overrightarrow{i_{rn}}\end{bmatrix}$ are the currents of the WPM coils; $\overrightarrow{\boldsymbol{i_o}} = \begin{bmatrix}\overrightarrow{i_{o1}}\\ \vdots\\ \overrightarrow{i_{om}}\end{bmatrix}$ are the receiver currents; $\boldsymbol{M_{io}} = [M_{io1} \quad \dots \quad M_{iom}]$ are the mutual inductances between the transmitter and receiver coils; $\boldsymbol{M_{ir}} = [M_{ir1} \quad \dots \quad M_{irn}]$ are the mutual inductances between the transmitter and WPM coils; $\boldsymbol{M_{oo}} = \begin{bmatrix}0 & \dots & M_{om1}\\ \vdots & \ddots & \vdots\\ M_{o1m} & \dots & 0\end{bmatrix}$ are the mutual inductances between the receiver coils; $\boldsymbol{M_{or}} = \begin{bmatrix}M_{o1r1} & \dots & M_{o1rn}\\ \vdots & \ddots & \vdots\\ M_{omr1} & \dots & M_{omrn}\end{bmatrix}$ are the mutual inductances between the receiver and WPM coils; $\boldsymbol{M_{rr}} = \begin{bmatrix}0 & \dots & M_{rn1}\\ \vdots & \ddots & \vdots\\ M_{r1n} & \dots & 0\end{bmatrix}$ are the mutual inductances between the WPM coils. Due to the exchange invariance of mutual inductance between the coils, $\boldsymbol{M_{ri}} = \boldsymbol{M_{ir}}^T$, $\boldsymbol{M_{oi}} = \boldsymbol{M_{io}}^T$ and $\boldsymbol{M_{ro}} = \boldsymbol{M_{or}}^T$. Besides, the voltages and currents of the WPM coils satisfy

$$\overrightarrow{\boldsymbol{v_r}} = \boldsymbol{Z_r}\overrightarrow{\boldsymbol{i_r}} \quad (2)$$

where $\boldsymbol{Z_r} = \begin{bmatrix}Z_{r1} & \dots & 0\\ \vdots & \ddots & \vdots\\ 0 & \cdots & Z_{rn}\end{bmatrix}$ is the diagonal matrix of the impedances of the WPM.

Based on (1) and (2), the voltages across the receiver coils can be derived by eliminating the electric variables of the WPM coils, i.e., $\overrightarrow{\boldsymbol{v_r}}$ and $\overrightarrow{\boldsymbol{i_r}}$,

$$\overrightarrow{\boldsymbol{v_o}} = j\omega(\boldsymbol{M_{oi}}\overrightarrow{i_i} - \boldsymbol{M_{oo}}\overrightarrow{\boldsymbol{i_o}}) + \omega^2\boldsymbol{M_{or}}(\boldsymbol{Z_r} + j\omega\boldsymbol{M_{rr}})^{-1}(\boldsymbol{M_{ri}}\overrightarrow{i_i} - \boldsymbol{M_{ro}}\overrightarrow{\boldsymbol{i_o}}) \quad (3)$$

By only considering the mutual couplings among the receivers and WPM (i.e., $\overrightarrow{i_i} = 0$), the transimpedances of $\overrightarrow{\boldsymbol{v_o}}$ over $\overrightarrow{\boldsymbol{i_o}}$ (i.e., $\boldsymbol{Z_{oo}}$) can be further derived based on (3) as

$$\boldsymbol{Z_{oo}} = -j\omega\boldsymbol{M_{oo}} - \omega^2\boldsymbol{M_{or}}(\boldsymbol{Z_r} + j\omega\boldsymbol{M_{rr}})^{-1}\boldsymbol{M_{ro}} \quad (4)$$

Note that $\boldsymbol{Z_{oo}}$ can be modulated via the proper design of the impedances and positions of the WPM.

III. Design Guidelines for WPM

To simplify the analysis without loss of generality, an SS-compensated WPT system with one transmitter, two receivers and one WPM is studied for the WPM designs. The placements of the coils are depicted in Fig. 3. The transmitter coil and WPM coil are placed on the straight center line in a co-axial manner. The two receiver coils are placed separately on the two sides of the central axis. The distances from the original point (i.e., *O*) to the transmitter, receiver, and WPM coils are labelled as d_1, d_2, d_3, and d_4, respectively. Therefore, d_4>0 indicate that the WPM coil is placed at the right side of the receiver coils, and vice versa. The receiver coils are not only magnetically coupled to the transmitter with the mutual inductances of M_{io1} and M_{io2}, but are also mutually coupled with the mutual inductances of M_{o1o2} and M_{o2o1} (i.e., $M_{o1o2} = M_{o2o1}$). The WPM coil, which is designed with an inductive-dominant impedance, is placed between the two receiver coils. The mutual inductances between the WPM coil and receive coils are M_{ro1} and M_{ro2}. The mutual inductance between the transmitter and WPM coils are negligible (i.e., $M_{ir} \approx 0$).

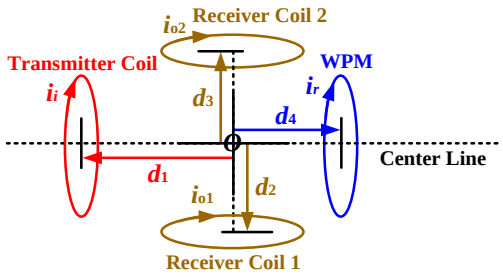

Fig. 3. Placements of the coils of the single-transmitter-two-receiver WPT system with a WPM.

Assume the impedance of the WPM is

$$Z_r = j\omega L_r + \frac{1}{j\omega C_r} \tag{5}$$

where C_r is the compensated capacitance. The impedance of the WPM can also be written as $Z_r = \frac{1}{\omega C_r}\left(\frac{\omega^2}{\omega_r^2} - 1\right)j$. Here, the resonant frequency of the WPM (i.e., ω_r) is smaller than the operating frequency (i.e., $\omega_r<\omega$), such that the impedance is inductive when the WPT system operates at the frequency of ω. Then, the transimpedances of the induced voltage on the receiver coil 1 by the receiver coil 2 and WPM coil (i.e., $\overrightarrow{v_{o1\_o2}} + \overrightarrow{v_{o1\_r}}$) over $\overrightarrow{\iota_{o2}}$, and the induced voltage on the receiver coil 2 by the receiver coil 1 and WPM coil (i.e., $\overrightarrow{v_{o2\_o1}} + \overrightarrow{v_{o2\_r}}$) over $\overrightarrow{\iota_{o1}}$ can be derived based on (4) and (5) as

$$Z_{o_1o_2} = \frac{\overrightarrow{v_{o1\_o2}}+\overrightarrow{v_{o1\_r}}}{\overrightarrow{\iota_{o2}}} = -j\omega M_{o_1o_2} - \frac{\omega^2 M_{ro_1} M_{ro_2}}{j\omega L_r + \frac{1}{j\omega C_r}} \tag{6}$$

$$Z_{o_2o_1} = \frac{\overrightarrow{v_{o2\_o1}}+\overrightarrow{v_{o2\_r}}}{\overrightarrow{\iota_{o1}}} = -j\omega M_{o_2o_1} - \frac{\omega^2 M_{ro_1} M_{ro_2}}{j\omega L_r + \frac{1}{j\omega C_r}} \tag{7}$$

According to (6) and (7), the transimpedances $Z_{o_1o_2}$ and $Z_{o_2o_1}$ are equal, which satisfy

$$-jZ_{o_1o_2}(\text{or } -jZ_{o_2o_1}) < 0 \quad \text{when } M_{ro_1}M_{ro_2} < M_{o_1o_2}L_r\left(1-\frac{\omega_r^2}{\omega^2}\right) \tag{8.1}$$

$$-jZ_{o_1o_2}(\text{or } -jZ_{o_2o_1}) = 0 \quad \text{when } M_{ro_1}M_{ro_2} = M_{o_1o_2}L_r\left(1-\frac{\omega_r^2}{\omega^2}\right) \tag{8.2}$$

$$-jZ_{o_1o_2}(\text{or } -jZ_{o_2o_1}) > 0 \quad \text{when } M_{ro_1}M_{ro_2} > M_{o_1o_2}L_r\left(1-\frac{\omega_r^2}{\omega^2}\right) \tag{8.3}$$

- Without the WPM (as shown in Fig. 4(a)), the magnetic flux density of the receiver coils (i.e., $\overrightarrow{B_O}$) can weaken the magnetic flux density of the transmitter coil (i.e., $\overrightarrow{B_i}$).
- When the WPM is placed at the position-1 (as shown in Fig. 4(b)), the mutual inductances between the receiver coils and WPM coil satisfy $M_{ro_1}M_{ro_2} < M_{o_1o_2}L_r\left(1-\frac{\omega_r^2}{\omega^2}\right)$. $\overrightarrow{B_O}$ is weakened by the magnetic flux density of the WPM coil (i.e., $\overrightarrow{B_r}$) but it still dominates. Consequently, the resultant magnetic flux density $\overrightarrow{B_O} + \overrightarrow{B_r}$ weakens $\overrightarrow{B_i}$. Therefore, $-jZ_{o_1o_2}(\text{or } -jZ_{o_2o_1}) < 0$ indicates the weakening of resultant magnetic flux density $\overrightarrow{B_O} + \overrightarrow{B_r}$ on $\overrightarrow{B_i}$. Compared to the weakening of $\overrightarrow{B_O}$ on $\overrightarrow{B_i}$ without the WPM, the weakening of resultant magnetic flux density $\overrightarrow{B_O} + \overrightarrow{B_r}$ on $\overrightarrow{B_i}$ is mitigated.
- When the WPM is moved from the position-1 to position-2 (as shown in Fig. 4(c)), the mutual inductances between the receiver coils and WPM coil increase and satisfy $M_{ro_1}M_{ro_2} = M_{o_1o_2}L_r\left(1-\frac{\omega_r^2}{\omega^2}\right)$. $\overrightarrow{B_O}$ is nullified by $\overrightarrow{B_r}$. Hence, $-jZ_{o_1o_2}(\text{or } -jZ_{o_2o_1}) = 0$ indicates $\overrightarrow{B_O} + \overrightarrow{B_r} = 0$. The magnetic coupling between the two receivers is eliminated by the WPM.
- When the WPM is further moved from the position-2 to position-3 (as shown in Fig. 4(d)), the mutual inductances between the receiver coils and WPM coil further increase and satisfy $M_{ro_1}M_{ro_2} > M_{o_1o_2}L_r\left(1-\frac{\omega_r^2}{\omega^2}\right)$. $\overrightarrow{B_r}$ dominates $\overrightarrow{B_O}$. As a result, the resultant magnetic flux density $\overrightarrow{B_O} + \overrightarrow{B_r}$ strengthens $\overrightarrow{B_i}$. Thus, $-jZ_{o_1o_2}(\text{or } -jZ_{o_2o_1}) > 0$ indicates the strengthening of resultant magnetic flux density $\overrightarrow{B_O} + \overrightarrow{B_r}$ on $\overrightarrow{B_i}$. Accordingly, the output power of the receivers can be enhanced.

In general, the output power of the receivers can be modulated by changing the mutual inductances between the receiver coils and the WPM.

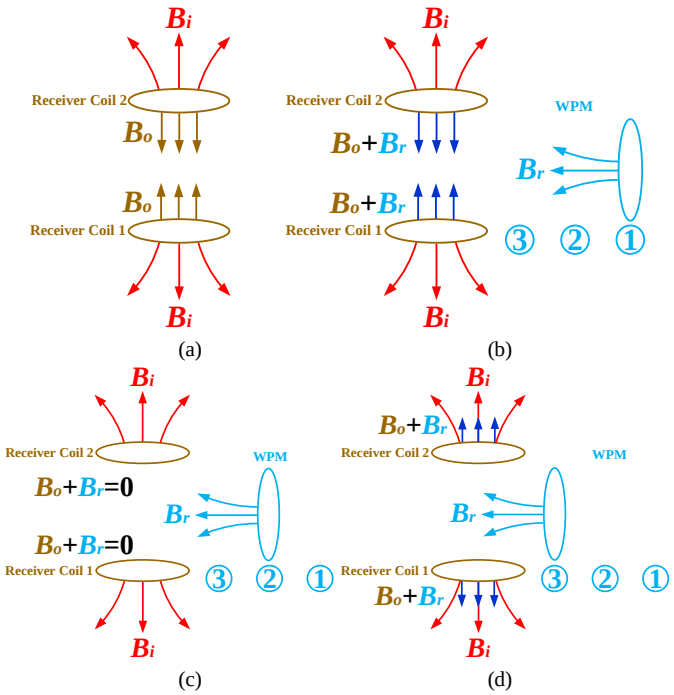

Fig. 4. Diagrams illustrating the magnetic flux density of the coils.

Based on (8), the curves of $-jZ_{o_1o_2}(\text{or } -jZ_{o_2o_1})$ versus $M_{ro_1}M_{ro_2}$ for three WPMs with different resonant frequencies can be plotted as shown in Fig. 5. Three conclusions can be drawn from the diagram:

- For the WPMs with different resonant frequencies, the term $-jZ_{o_1o_2}(\text{or } -jZ_{o_2o_1})$ will be increased when the mutual inductances between the receiver coils and the WPM coil are increased.
- For a WPM with a higher resonant frequency (i.e., $\omega_{r3} > \omega_{r2} > \omega_{r1}$), the power decoupling point (i.e.,$M_{ro_1}M_{ro_2} = M_{o_1o_2}L_r\left(1-\frac{\omega_r^2}{\omega^2}\right)$) is closer from the original point (i.e., O).
- Based on (6) and (7), for the WPM with a fixed impedance,

$$\frac{\partial(-jZ_{o_1o_2})}{\partial(M_{ro_1}M_{ro_2})} = \frac{\partial(-jZ_{o_2o_1})}{\partial(M_{ro_1}M_{ro_2})} = \frac{\omega^3}{L_r(\omega^2-\omega_r^2)} \tag{9}$$

Here, $\frac{\omega^3}{L_r(\omega^2-\omega_r^2)}$ indicate the slopes of the curves in Fig. 5. Apparently, the slope of the curve is greater for the WPM with a higher resonant frequency (i.e., $\omega_{r3} > \omega_{r2} > \omega_{r1}$). This indicates that the change of the output power is more prominent when the WPM with a higher resonant frequency is moved toward or away from the original point (i.e., *O*).

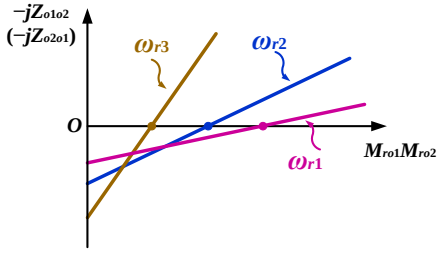

Fig. 5. The curves of $-jZ_{o_1o_2}$(or $-jZ_{o_2o_1}$) versus $M_{ro_1}M_{ro_2}$.

IV. Experimental Verifications

Experiments are conducted on a 20 W single-transmitter-double-receiver WPT system with a WPM, as shown in Fig. 6. The input DC voltage of the WPT system is 3.3 V. The WPT system operates at 100 kHz. A class-D power amplifier is used to drive the transmitter coil. The TMS32F28335 digital signal processor (DSP) from Texas Instrument (TI) is used as the controller for the class-D power amplifier. All the transmitter coil, receiver coils, and the WPM coil are wounded by Litz wires. The specifications of the coils are given in Table I. The rated power of the two LED loads is 3.6 W.

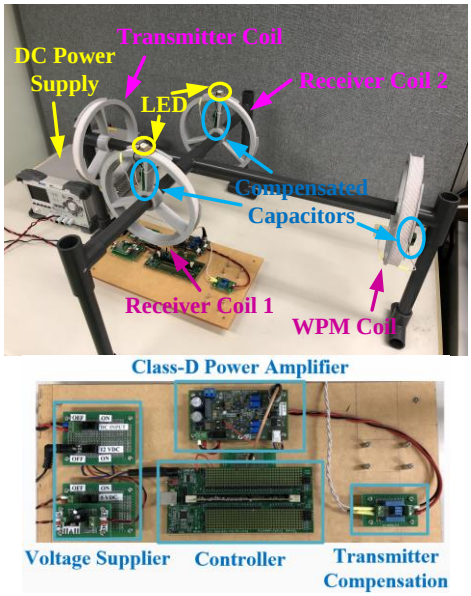

Fig. 6. Photograph of the experimental setup.

TABLE I. Main Specificaitons of the Coils

Description	Symbol	Value
Diameter of the transmitter coil	D_i	20 cm
Number of turns of the transmitter coil	N_i	11
Diameter of the receiver coil 1	D_{o1}	20 cm
Number of turns of the receiver coil 1	N_{o1}	11
Diameter of the receiver coil 2	D_{o2}	20 cm
Number of turns of the receiver coil 2	N_{o2}	11
Diameter of the WPM coil	D_r	20 cm
Number of turns of the WPM coil	N_r	11
Inductance of the transmitter coil	L_i	49.261 μH
Compensated capacitance of the transmitter coil	C_i	53 nF
ESR of the transmitter coil	R_i	0.177 Ω
Inductance of the receiver coil 1	L_{o1}	49.262 μH
Compensated capacitance of the receiver coil 1	C_{o1}	52.7 nF
ESR of the receiver coil 1	R_{o1}	0.214 Ω
Inductance of the receiver coil 2	L_{o2}	49.254 μH
Compensated capacitance of the receiver coil 2	C_{o2}	52.7 nF
ESR of the receiver coil 2	R_{o2}	0.159 Ω
Inductance of the WPM coil	L_r	48.087 μH
ESR of the WPM coil	R_r	0.169 Ω

Initially, the WPT system operates at the nominal condition (i.e., d_1=25 cm, d_2=d_3=13 cm, and the WPM resonant frequency is 95 kHz), while the WPM is moved from d_4=16 cm to d_4=4 cm. The corresponding magnetic flux of the coils at the positions of d_4=16 cm and d_4=4 cm is similar to the case in Fig. 4(b), while it is similar to the case in Fig. 4(d) at the position of d_4=9.4 cm. According to the analysis, the output power of the LED loads at the position of d_4=9.4 cm is larger than the power at the positions of d_4=16 cm and d_4=4 cm. Fig. 7 show the experimental results of the nominal WPT system with the WPM at the positions of d_4=4 cm, d_4=9.4 cm, and d_4=16 cm, respectively. Compared to the brightness of the LED loads in Figs. 7(a) and (c), the brightness of the LED loads in Fig. 7(b) are much higher, which validates the analysis in Fig. 5.

(a) d_4=4 cm

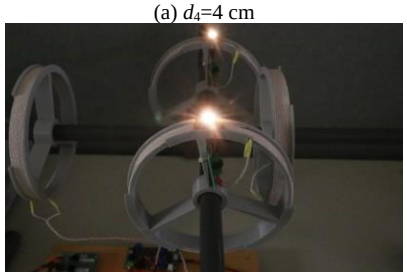

(b) d_4=9.4 cm

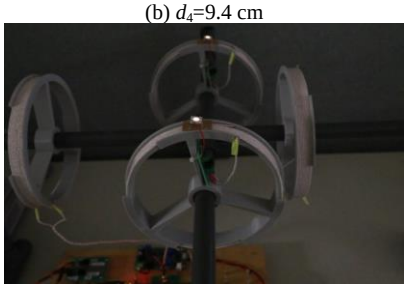

(c) d_4=16 cm

Fig. 7. Experimental results of the nominal WPT system with the WPM coil at different positions.

Then, the WPT system is operated with fixed positions of all the coils (i.e., d_1=25 cm, d_2=d_3=13 cm, and d_4=9.4 cm), while the resonant frequency of the WPM is changed from 90 kHz, to 95 kHz, and then to 99 kHz. Fig. 8 shows the experimental results of the WPT system with the WPM at the resonant frequency of 90 kHz, 95 kHz, and 99 kHz, respectively. Clearly, the brightness of the two LED loads increases when the resonant frequency of the WPM increases, which verifies the analysis in Fig. 5.

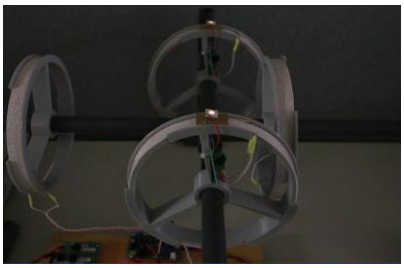

(a) f_r=90 kHz

(b) f_r=95 kHz

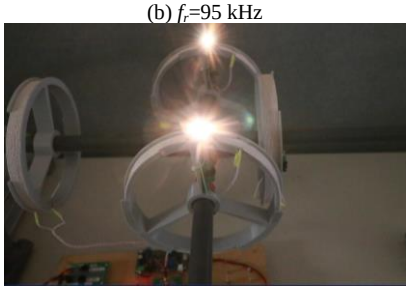

(c) f_r=99 kHz

Fig. 8. Experimental results of the WPT system with the WPM coil at different resonant frequencies.

V. Conclusions

A general power modulation principle for single-transmitter-multiple-receiver wireless power transfer (WPT) systems is proposed in this paper. It is shown that inductive-dominant relay resonators can be used as wireless power modulators (WPMs) for WPT systems with multiple receivers. Based on the principle, a design method of the WPM for a 20 W single-transmitter-two-receiver WPT system is presented. Experimental results verify that the designed WPM can regulate the output power of the system via the modulation of the magnetic coupling between the receiver coils.

Acknowledgement

This work was supported by the Start-up Fund for RAPs under the Strategic Hiring Scheme of PolyU P0036194.

References

[1] S. Chen, Y. Wang, and S. Chung, "A decoupling technique for increasing the port isolation between two strongly coupled antennas", *IEEE Trans. Anten. Prop.*, vol. 56, no.12, pp. 3650-3658, Dec. 2008.

[2] E. J. Wilkinson, "An N-way hybrid power divider," *IRE Trans. Micro. Theory and Technol*., vol. 8, no. 1, pp. 116-118, Jan. 1960.

[3] Y. Ohta, R. Ishikawa, and K. Honjo, "A 5.8-GHz reconfigurable power diver for wireless power transfer," in *Proc. of Asia-Pacific Microwave Conf.*, pp. 693- 695, 2014.

[4] Qi standard v.1.2.3, Feb, 2017, Wireless power consortium.

[5] AirFuel Alliance: https://www.airfuel.com/.

[6] SAE J2954 Standard, May 2016, Society of Automobile Engineers.

[7] S. Y. R. Hui, W. Zhong; C. K. Lee, "A critical review of recent progress in mid-range wireless power transfer," *IEEE Transactions on Power Electronics*, vol. 29, no. 9, pp. 4500-4511, 2014.

[8] C. Zheng, J. S. Lai, R. Chen, et. al., "High-efficiency contactless power transfer system for electric vehicle battery charging application," *IEEE Trans. Emerg. Sel. Topics Power Electron.*, vol. 3, no. 1, pp. 65-74, Mar. 2015.

[9] J. Miller, O. Onar, and M. Chinthavali, "Primary-side power flow control of wireless power transfer for electric vehicle charging," *IEEE Trans. Emerg. Sel. Topics Power Electron.*, vol. 3, no. 1, pp. 147-162, Mar. 2015.

[10] I. Nam, R. Dougal, and E. Santi, "Novel control approach to achieving efficient wireless battery charging for portable electronic devices," in *2012 IEEE Energy Conversion Congress and Exposition (ECCE)*, pp. 2482-2491, Sept. 2012.

[11] Z. Li, K. Song, J. Jiang, and C. Zhu, "Constant current charging and maximum efficiency tracking control scheme for supercapacitor wireless charging," *IEEE Trans. Power Electron.*, vol. 33, no. 10, pp. 9088-9100, Oct. 2018.

[12] Y. Li, J. Hu, F. Chen, Z. Li, Z. He, and R. Mai, "Dual-phase-shift control scheme with current-stress and efficiency optimization for wireless power transfer systems," *IEEE Trans. Circuits Syst. I, Reg. Papers*, vol. 65, no. 9, pp. 3110–3121, Sept. 2018.

[13] W. Zhong and S. Y. R. Hui, "Maximum energy efficiency tracking for wireless power transfer systems with dynamic coupling coefficient estimation," *IEEE Trans. Power Electron*., vol. 30, no. 6, pp. 5005–5015, Jul. 2015.

[14] W. Zhong and S. Y. R. Hui, "Maximum energy efficiency operation of series-series resonant wireless power transfer systems using on-off keying modulation," *IEEE Trans. Power Electron*., vol. 33, no. 4, pp. 3595–3603, Apr. 2018.

[15] Y. Yang, W. Zhong, S. Kiratipongvoot, S. C. Tan, and S. Y. R. Hui, "Dynamic improvement of series-series compensated wireless power transfer systems using discrete sliding mode control," *IEEE Trans. Power Electron*., vol. 33, no. 7, pp. 6351–6360, Jul. 2018.

[16] Y. Yang, S. C. Tan, and S. Y. R. Hui, "Communication-free control scheme for Qi-compliant wireless power transfer systems," in *IEEE Energy Conversion Congress and Exposition (ECCE)*, pp. 4955–4960, Sept. 2019.

[17] K. Colak, E. Asa, M. Bojarski, D. Czarkowski, and O. Onar, "A novel phase-shift control of semibridgeless active rectifier for wireless power transfer," *IEEE Trans. Power Electron*., vol. 30, no. 11, pp. 6288–6297, Nov. 2015.

[18] X. Dai, X. Li, Y. Li, and A. P. Hu, "Maximum efficiency tracking for wireless power transfer systems with dynamic coupling coefficient estimation," *IEEE Trans. Power Electron*., vol. 30, no. 6, pp. 5005–5015, Jun. 2018.

[19] Z. Huang, S. C. Wong, and C. K. Tse, "Control design for optimizing efficiency in inductive power transfer systems," *IEEE Trans. Power Electron*., vol. 33, no. 5, pp. 4523–4534, May 2018.